frontiers in Chemistry

ORIGINAL RESEARCH
published: 21 May 2019
doi: 10.3389/fchem.2019.00312

Pyrazine-Based Blue Thermally Activated Delayed Fluorescence Materials: Combine Small Singlet–Triplet Splitting With Large Fluorescence Rate

Junyuan Liu†, Keren Zhou†, Dan Wang, Chao Deng, Ke Duan, Qi Ai and Qisheng Zhang**

MOE Key Laboratory of Macromolecular Synthesis and Functionalization, Department of Polymer Science and Engineering, Zhejiang University, Hangzhou, China

OPEN ACCESS

Edited by:
Lian Duan,
Tsinghua University, China

Reviewed by:
Zujin Zhao,
South China University of Technology, China
Bing Yang,
Jilin University, China

***Correspondence:**
Qi Ai
0617289@zju.edu.cn
Qisheng Zhang
qishengzhang@zju.edu.cn

†These authors have contributed equally to this work

Specialty section:
This article was submitted to Organic Chemistry, a section of the journal Frontiers in Chemistry

Received: *27 February 2019*
Accepted: *18 April 2019*
Published: *21 May 2019*

Citation:
Liu J, Zhou K, Wang D, Deng C, Duan K, Ai Q and Zhang Q (2019) Pyrazine-Based Blue Thermally Activated Delayed Fluorescence Materials: Combine Small Singlet–Triplet Splitting With Large Fluorescence Rate. Front. Chem. 7:312. doi: 10.3389/fchem.2019.00312

Metal-free thermally activated delayed fluorescence (TADF) emitters have emerged as promising candidate materials for highly efficient and low-cost organic light-emitting diodes (OLEDs). Here, a novel acceptor 2-cyanopyrazine is selected for the construction of blue TADF molecules via computer-assisted molecular design. Both theoretical prediction and experimental photophysical data indicate a small S_1-T_1 energy gap (ΔE_{ST}) and a relative large fluorescence rate (k_F) in an *o*-phenylene-bridged 2-cyanopyrazine/3,6-di-*tert*-butylcarbazole compound (TCzPZCN). The k_F value of 3.7×10^7 s^{-1} observed in a TCzPZCN doped film is among the highest in the TADF emitters with a ΔE_{ST} smaller than 0.1 eV. Blue TADF emission is observed in a TCzPZCN doped film with a short TADF lifetime of 1.9 μs. The OLEDs using TCzPZCN as emitter exhibit a maximum external quantum efficiency (EQE) of 7.6% with low-efficiency roll-off. A sky-blue device containing a derivative of TCzPZCN achieves an improved EQE maximum of 12.2% by suppressing the non-radiative decay at T_1.

Keywords: thermally activated delayed fluorescence (TADF), pyrazine, blue organic light-emitting diodes (OLED), fluorescence rate constant, singlet-triplet splitting

INTRODUCTION

Owing to the small energy gap (ΔE_{ST}) between the lowest singlet (S_1) and triplet (T_1) excited states, metal-free thermally activated delayed fluorescence (TADF) molecules can upconvert from their T_1 to S_1 by absorbing environmental thermal energy and then decay radiatively from the S_1. Organic light-emitting diodes (OLEDs) employing TADF emitters can convert both singlet and triplet excitons into light with a theoretical yield up to 100% (Wex and Kaafarani, 2017; Yang et al., 2017; Cai and Su, 2018; Cai et al., 2018; Liu Y. et al., 2018), and have emerged as a new representation for highly efficient and low-cost OLEDs (Liu et al., 2014; Li W. et al., 2014; Ai et al., 2018; Bian et al., 2018). A twisted donor–phenylene–acceptor (D-Ph-A) structure has been demonstrated to be an effective strategy for the design of TADF materials (Zhang et al., 2012). A number of efficient blue, green, and red TADF materials with small ΔE_{ST} have been developed by using this strategy in recent years (Uoyama et al., 2012; Wang et al., 2014, 2017; Zhang et al., 2014a,b; Chen et al., 2016; Chen X.-L. et al., 2017; Li et al., 2017; Yuan et al., 2017; Wu et al., 2018; Zhang D. et al., 2018).

Except for ΔE_{ST}, the value of fluorescence rate (k_F) for TADF emitters has attracted more and more attention in recent years, because it is a key for not only the quantum efficiency of the emitter but also the TADF lifetime and the device stability (Zhang et al., 2014a,b; Liu Z. et al., 2018). The D-Ph-A-type TADF emitters with small twisting angles between the neighboring planes can have high k_F values but suffer from large ΔE_{ST}, which leads to significant efficiency roll-off in their devices (Zhang et al., 2012; Li et al., 2013; Hirata et al., 2015; Chen X.-K. et al., 2017). Although increasing the twisting angle can reduce ΔE_{ST}, the k_F value also decreases due to the reduced overlap of the orbitals involved in the S_1 transition (Zhang et al., 2014a). Especially, for blue TADF emitters with large band gaps, large twisting angle cannot ensure a small ΔE_{ST}, because the molecules may have a low-lying triplet state localized at the D or A moieties (Zhang et al., 2014b). Overall, the difficulty of TADF material design is to have small ΔE_{ST} and high k_F at the same time. To enlarge the ratio of k_F to ΔE_{ST}, the D-A couple should be carefully selected, and the twisting geometry should be well-designed.

Cyano (Uoyama et al., 2012; Li B. et al., 2014; Lee and Lee, 2015; Taneda et al., 2015; Zhang et al., 2016; Chan et al., 2018; Sommer et al., 2018) and aromatic imines [i.e., triazine (Endo et al., 2011; Lee et al., 2012; Tanaka et al., 2012; Hirata et al., 2015; Kaji et al., 2015; Cha et al., 2016; Lin et al., 2016; Zhu et al., 2016; Chen X.-K. et al., 2017; Cui et al., 2017; Shao et al., 2017; Liu Z. et al., 2018; Oh et al., 2018; Zhang Q. et al., 2018; Wang Q. et al., 2019; Zhang et al., 2019) pyrimidine (Gómez-Bombarelli et al., 2016; Komatsu et al., 2016; Pan et al., 2016; Wu et al., 2016; Ganesan et al., 2017; Nakao et al., 2017; Park et al., 2017; Xiang et al., 2017; Zhang Q. et al., 2018; Zhang et al., 2019), and pyridine (Tang et al., 2015; Pan et al., 2016; Rajamalli et al., 2017; Sasabe et al., 2017; Chen et al., 2018)] are the most used groups for the construction of acceptor moieties in TADF molecules. The electron-withdrawing capability of an aromatic imine increases with an increase in the number of nitrogen atoms in the ring. 2,4,6-Triphenyl-1,3,5-triazine (TRZ) is a promising acceptor for blue and green TADF materials because of the high T_1 energy level and the relatively strong electron-withdrawing capability (Tanaka et al., 2012; Hirata et al., 2015; Kaji et al., 2015; Cha et al., 2016; Lin et al., 2016; Chen X.-K. et al., 2017; Cui et al., 2017; Shao et al., 2017; Liu Z. et al., 2018; Oh et al., 2018; Zhang D. et al., 2018; Wang Q. et al., 2019). The aromatic heterocyclic rings containing one or two imine groups have a relatively weak electron-withdrawing character, which can be strengthened by introducing additional cyano groups (Tang et al., 2015; Pan et al., 2016; Sasabe et al., 2017; Chen et al., 2018). Although a series of red fluorophores based on pyrazine-2,3-dicarbonitrile has been reported (Gao et al., 2006), the pyrazine-based acceptor hasn't been used to construct a TADF molecule so far. In this paper, the T_1 energy levels and reduction potentials of various cyano-substituted pyrazines are theoretical investigated. A blue TADF emitter with small ΔE_{ST} and relatively large k_F values is successfully designed and synthesized by employing 2-cyanopyrazine as the acceptor.

RESULTS AND DISCUSSION

The CT transition energy is significantly related to the electron-donating ability of the donor and the electron-withdrawing ability of the acceptor in a D-A molecule. To avoid a low-lying locally excited triplet state (^{3}LE) existing under the S_1 (^{1}CT), both donor and acceptor moieties should have a limited conjugation length, and the conjugation between donor and acceptor should be broken (Zhang et al., 2014b). The electron-withdrawing capability of pyrazine is weaker than that of 1,3,5-triazine, which is an ideal acceptor for blue and green TADF materials. To enhance the electron-withdrawing capability of pyrazine, one to three cyano groups are attached onto the pyrazine ring in 2-phenylpyrazine, in which the phenyl ring is used as a π-bridge between the donor and acceptor moieties. The

TABLE 1 | Computed vertical absorption energies (E_{VA}), zero–zero energies (E_{0-0}), lowest unoccupied molecular orbital energies (E_{LUMO}), and reduction potentials (E_{RED}) of cyano-substituted triazine, pyrimidine, and pyridine moieties.

No.	1	2	3	4	5	6	7	TRZ
Molecular structure[a]	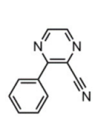	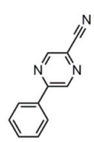	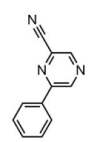	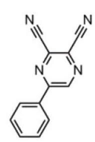	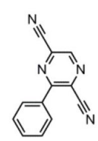	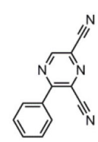	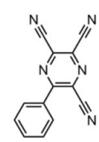	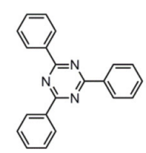
$E_{VA}(T_1)$ (eV)[b]	3.03	2.72	2.95	2.63	2.74	2.78	2.57	3.02
$E_{0-0}(T_1)$ (eV)[c]	2.88	2.58	2.80	2.49	2.59	2.60	2.42	2.87
E_{LUMO} (eV)[d]	−2.45	−2.71	−2.52	−3.18	−3.37	−3.13	−3.81	−2.05
E_{RED} (V)[e]	2.94	3.14	2.99	3.51	3.66	3.47	4.01	2.63

[a] *The geometries are optimized via DFT at the B3LYP/6-311G(d,p) level in vacuum.*

[b] *Calculated by TD-DFT/B3LYP/6-31G(d) in vacuum.*

[c] *Calculated from $E_{VA}(T_1)$ with a correlation of $E_{0-0}(T_1) = E_{VA}(T_1)/1.02 - 0.09$ (Huang et al., 2013).*

[d] *Derived from DFT/PBE0/6-311++G(d,p) in acetonitrile.*

[e] *Referred to an electron in the vacuum state (Mazur and Hipps, 1995) and calculated from the E_{LUMO} with a correlation of $E_{RED} = 0.79 \times (-E_{LUMO}) + 1.01$ (Wang D. et al., 2019).*

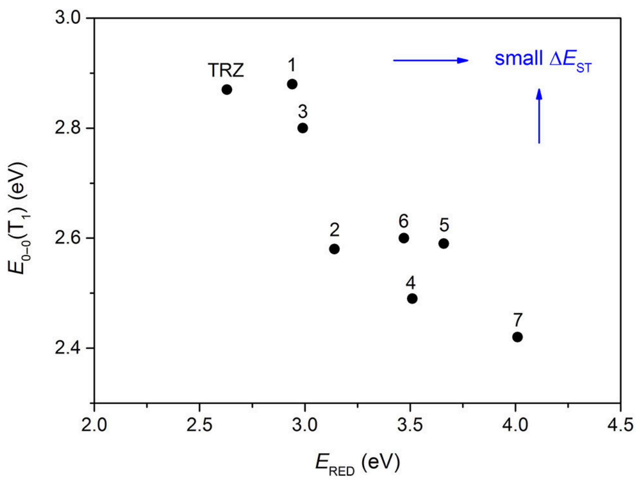

FIGURE 1 | Correlation of calculated $E_{0-0}(T_1)$ and E_{RED}. The structures of the molecules are shown in **Table 1**.

calculated zero–zero energy of T_1 [$E_{0-0}(T_1)$] and the reduction potentials (E_{RED}) of the substituted pyrazine fragments are listed in **Table 1** and compared with those of TRZ (Mazur and Hipps, 1995; Huang et al., 2013; Wang D. et al., 2019). As shown in **Figure 1**, there is a roughly proportional relationship between $E_{0-0}(T_1)$ and E_{RED}, i.e., reducing the conjugation length of a moiety generally decreases its electron-withdrawing capability. The theoretical $E_{0-0}(T_1)$ of 3-phenylpyrazine-2-carbonitrile (Liu Y. et al., 2018) (2.88 eV) is as high as that of TRZ (2.87 eV), while the electron-withdrawing capability of **1** ($E_{RED} = 2.94$ eV) is even higher than that of TRZ ($E_{RED} = 2.63$ eV) (Mazur and Hipps, 1995), indicating that 2-cyanopyrazine is a promising acceptor for blue and green TADF molecules.

Using 3-phenylpyrazine-2-carbonitrile (Liu Y. et al., 2018) as the π-bridge attached acceptor and 3,6-di-tertbutylcarbazole as the donor, two molecules TCzPZCN and 2TCzPZCN are designed (**Figure 2A**). TCzPZCN has only one 3,6-di-tertbutylcarbazole donor group, which links to the acceptor group 2-cyanopyrazine via the ortho position of the phenylene (Ph) bridge (Wang R. et al., 2018). The ground-state geometry of TCzPZCN is optimized by DFT/B3LYP/6-31G*. The dihedral angle between carbazole donor and Ph-bridge is 69°, while that between 2-cyanopyrazine acceptor and Ph-bridge is 55° (**Figure 2B**). Such moderate dihedral angles allow a small overlap of the orbitals involved in the CT transition on the Ph-bridge but effectively break the conjugation between the donor and the acceptor. For 2TCzPZCN, there are two 3,6-di-tertbutylcarbazole groups attached to the ortho and meta positions of the Ph-bridge. Although the meta-linked carbazole and the Ph-bridge have a relatively small dihedral angle of 52°, the meta linkage prevents the orbitals on the donor from extending to the acceptor (**Figure 2B**). Using the *K*-OHF method, a semiempirical descriptor selection method based on time-dependent DFT (Wang et al., 2018), the vertical absorption energies (E_{VA}) of TCzPZCN and 2TCzPZCN are calculated to be 3.15 and 3.16 eV, respectively. Assuming that their absorption is a 0–1 transition, the commonest transition for TADF emitters in weak polar medium, the $E_{0-0}(S_1)$ values of TCzPZCN and 2TCzPZCN in toluene are evaluated to be 2.91 and 2.92 eV, respectively (Huang et al., 2013). The ΔE_{ST} and the oscillator strength (f) are calculated to be 0.05 and 0.0157 for TCzPZCN, respectively, and 0.05 and 0.0184 for 2TCzPZCN, respectively. The ratios of f to ΔE_{ST} are among the highest values for the TADF emitters ($\Delta E_{ST} < 0.15$ eV) calculated using the *K*-OHF method (**Table S1**). Using a rough relationship between the theoretical frontier orbital energies and the measured redox potentials (Wang D. et al., 2019), the oxidation potentials (E_{OX}) of TCzPZCN and 2TCzPZCN are calculated to be 5.46 and 5.41 V, respectively, in dichloromethane, while the E_{RED} of TCzPZCN and 2TCzPZCN are calculated to be 2.90 and 2.98 V, respectively, in acetonitrile (**Table 2**).

TABLE 2 | A comparison of theoretical predictions and experimental data on photophysical and electrochemistry of the investigated molecules.

	Theoretical data		Experimental data	
	TCzPZCN	**2TCzPZCN**	**TCzPZCN**	**2TCzPZCN**
In Toluene				
$E_{VA}(S_1)$ (eV)	3.15	3.16		
$E_{0-0}(S_1)$ (eV)[a]	2.91	2.92	2.91	2.82
ΔE_{ST} (eV)	0.05	0.05	0.07	0.06
f[b]	0.0157	0.0184		
λ_{em} (nm)[c]			490	503
Φ[d]			0.10	0.05
$\tau_1/\tau_2/\tau_3$ (ns)			0.14/2.6/8.4	0.12/3.2/9.8
In mCP Film (10 wt%)				
λ_{em} (nm)			483	493
Φ/Φ_F			0.47/0.36	0.44/0.16
τ_F (ns)			9.7	7.2
τ_{TADF} (μs)			1.9	8.1
k_F ($\times 10^7$ s^{-1})			3.7	2.2
In Dichloromethane				
E_{OX} (V)[e]	5.46	5.41	5.57	5.53
In Acetonitrile				
E_{RED} (V)[e]	2.90	2.98	2.92	2.95

[a] *Calculated from $E_{VA}(S_1)$ with a correlation of $E_{0\text{-}0}(S_1) = E_{VA}(S_1) - 0.24$ eV (Huang et al., 2013).*
[b] *Oscillator strength.*
[c] *Emission maximum.*
[d] *Photoluminescence quantum yield.*
[e] *Referred to the vacuum state.*
*The theoretical potentials are calculated in the same way as those in **Table 1**.*

The synthesis of TCzPZCN and 2TCzPZCN is described in the **Supplementary Material**. Their absorption and emission spectra in toluene and 10 wt% *m*-bis(N-carbazolyl)benzene (mCP) films are presented in **Figure 3** and **Figure S1**. As shown in **Figure 3A**, the absorption shoulders in the wavelength region of 350–430 nm can be ascribed to the intramolecular charge-transfer (CT) transitions. The fluorescence (1–2 ns component) and phosphorescence (1–2 ms component) spectra in toluene at 77 K are all smooth and broad. The ΔE_{ST}

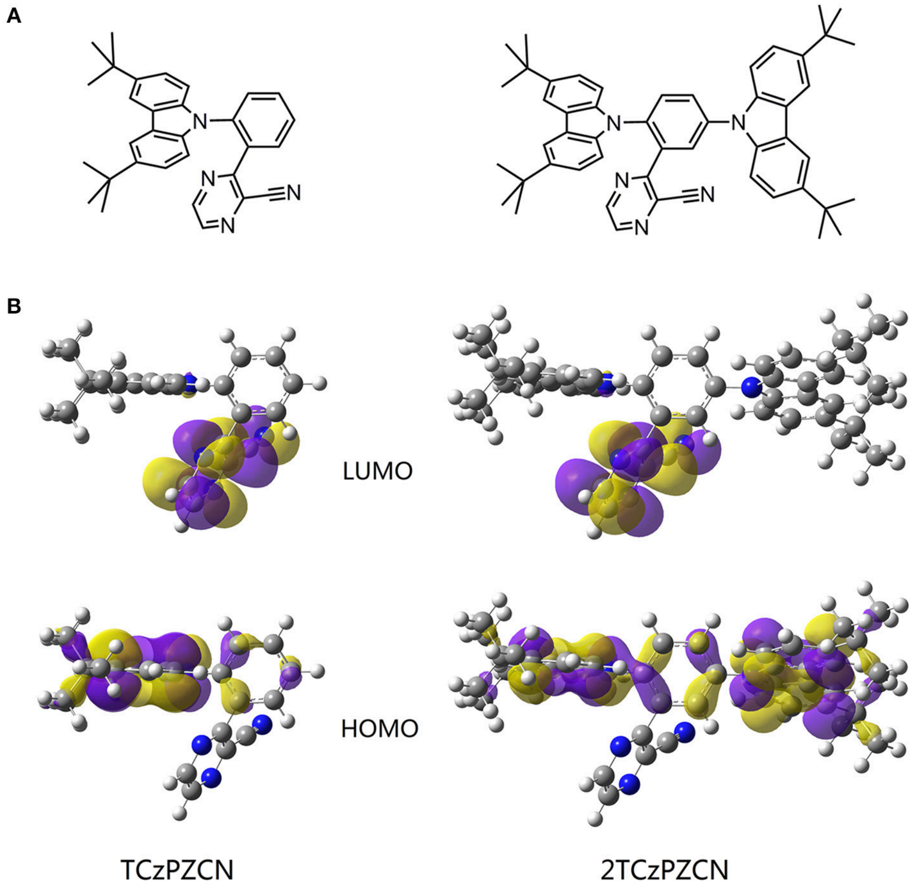

FIGURE 2 | (A) Structures of the investigated molecules. **(B)** The highest occupied and lowest unoccupied molecular orbitals (HOMO and LUMO) of the investigated molecules in their S0 state in vacuum. The geometries are optimized via density functional theory (DFT) at the B3LYP/6-311G (d,p) level.

values can be estimated from the energy difference between the fluorescence and phosphorescence peaks. The measured ΔE_{ST} of 0.07 eV for TCzPZCN and 0.06 eV for 2TCzPZCN are close to the theoretical values (**Table 2**). From the onset of the fluorescence bands at room temperature (RT; **Figure S1**), the 0–0 energies of TCzPZCN and 2TCzPZCN in toluene are estimated to be 2.91 and 2.82 eV, respectively, which are also in good agreement with the above theoretical estimation. These two compounds emit brightly at 77 K but dimly at RT with photoluminescence quantum yields (PLQY) <0.10 (**Figure 3A** inset and **Table 2**). In comparison to the emission spectra in solvent glass, those in the fluid solution (**Figure S1**) exhibit a significant redshift, indicating a correlation between the serious non-radiative decay in RT toluene and the excited-state geometrical relaxation process.

The transient decay spectra in degassed toluene at RT are presented in **Figure 3B**. No obvious TADF component is observed in the microsecond time range. Besides the single-exponential nanosecond fluorescence decay, a quick decay in the picosecond time scale is recorded by using an ultrafast time-correlated single photon counting (TCSPC). This fast decay could be resolved into two exponentially decaying components with the lifetimes (τ) of 0.14 and 2.6 ns for TCzPZCN and 0.12 and 3.2 ns for 2TCzPZCN. It is reasonable to expect that the non-radiative decay rate (k_{nr}) is not a constant during the fluorescence decay process. It is known that the excited-state solvation and relaxation process can be completed in a few picoseconds in fluid solution (Castner et al., 1987; Kinoshita and Nishi, 1988), resulting in a very fast non-radiative decay via a so-called free rotor and loose bolt effects (Turro et al., 2010). If the radiative and non-radiative decay rates are constants in the total luminescence process, the k_F value can be obtained by the following formula:

$$k_F = \Phi_F/\tau_F \quad (1)$$

where Φ_F and τ_F are the PLQY and lifetime of the fluorescence component, respectively. Given that both the k_F and k_{nr} in the first few nanoseconds are the same as the values after that, the PLQYs of these two compounds in toluene will be significantly higher than the observed ones. Consequently, if we calculate k_F from the measured Φ_F and the dominant nanosecond τ with Equation 1, the k_F value will be considerably underestimated.

In 10-wt%-doped mCP films, TCzPZCN and 2TCzPZCN exhibit blueshifted emission peaks at 483 and 493 nm, respectively (**Figure 3C**), with respect to that in toluene. Meanwhile, the PLQYs of TCzPZCN and 2TCzPZCN in the

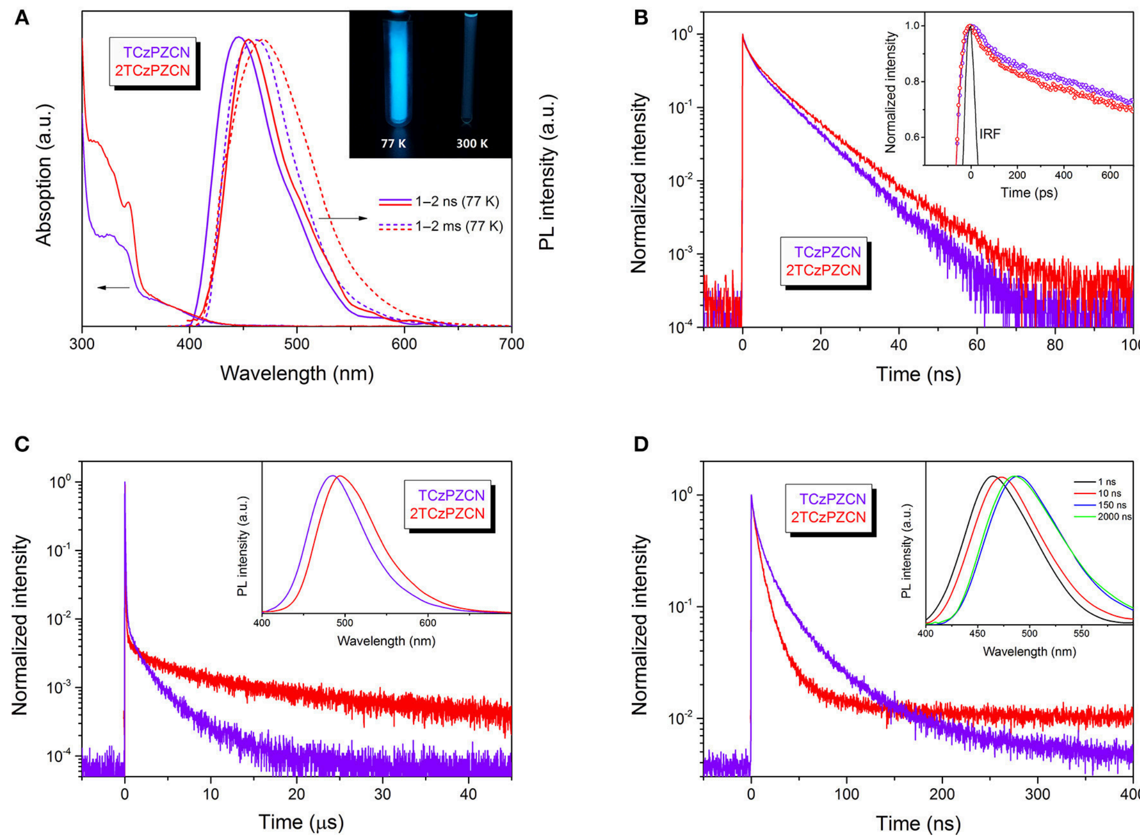

FIGURE 3 | Absorption, emission and transient decay spectra. **(A)** Absorption spectra of the investigated molecules in toluene at room temperature (RT), and fluorescence (1–2 ns) and phosphorescence (1–2 ms) spectra in toluene at 77 K. Inset: A comparison of TCzPZCN in toluene at 77 K and RT under 365-nm ultraviolet irradiation. **(B)** Transient decay spectra of the investigated molecules in toluene at RT. Inset: Instrument response function (IRF). **(C)** Transient decay spectra of the investigated molecules doped into mCP films (10 wt%) measured on a microsecond time scale at RT. Inset: Steady-state emission spectra of the doped films at RT. **(D)** Transient decay spectra of the investigated molecules doped into mCP films (10 wt%) measured on a nanosecond time scale at RT. Inset: Time-resolved emission spectroscopy of the TCzPZCN doped films at RT.

doped films increase to 0.47 and 0.44, respectively, owing to the suppression of the collision-induced non-radiative decay (Turro et al., 2010; Zhang et al., 2014a). However, it was previously demonstrated that there is enough free volume in amorphous organic semiconductor films (Sun et al., 2017). The large-amplitude excited-state distortion cannot be fully inhibited in the films, leading to the moderate PLQYs for these films. TADF decay can be observed from the doped films, with a short lifetime of 1.9 μs for TCzPZCN and 8.1 μs for 2TCzPZCN (**Figure 3C**).

It is known that the solvation effect increases the separation of the electron and hole in a CT state (Sun et al., 2017; Wang and Zhang, 2019) and consequently decreases the fluorescence rate. According to the time-resolved emission spectroscopy shown in **Figure 3D**, the solvation process in a doped mCP film can last for dozens of nanoseconds, which is much slower than that in fluid solutions (Deng et al., 2019). The fluorescence rate of a TADF emitter in organic thin films decreases gradually in this time region and therefore can have a higher average value than that in solution. Since the fluorescence decays in organic thin films are always best fit by multiple exponentials (**Figure 3D**), an average lifetime determined from the time the fluorescence intensity decays to 1/e of the initial value (**Table 2**) is used to calculate the k_F values. The k_F value of TCzPZCN in doped mCP films is then calculated to be 3.7×10^7 s^{-1}, which is considerably higher than those of the TADF emitters having a ΔE_{ST} smaller than 0.1 eV (**Table S2**). In comparison to TCzPZCN, 2TCzPZCN has a lower k_F of 2.2×10^7 s^{-1}, probably because of the reduced distance between the charge centroids of the donor and acceptor orbitals (**Figure 2**). According to first-principles calculation, the square root of the CT transition rate is approximately proportional to the effective D/A separation distance and the orbital overlap integral (Phifer and McMillin, 1986; Zhang et al., 2014a).

The oxidation and reduction behaviors of TCzPZCN and 2TCzPZCN are measured by cyclic voltammetry in dichloromethane and acetonitrile, respectively (**Figure S2**). From the onsets of the quasi-reversible redox couples, the vacuum-state-referenced E_{OX} and E_{RED} of TCzPZCN are determined to be 5.57 and 2.92 V, respectively, while those of 2TCzPZCN are determined to be 5.53 and 2.95 V, respectively. These potential values are all close to their

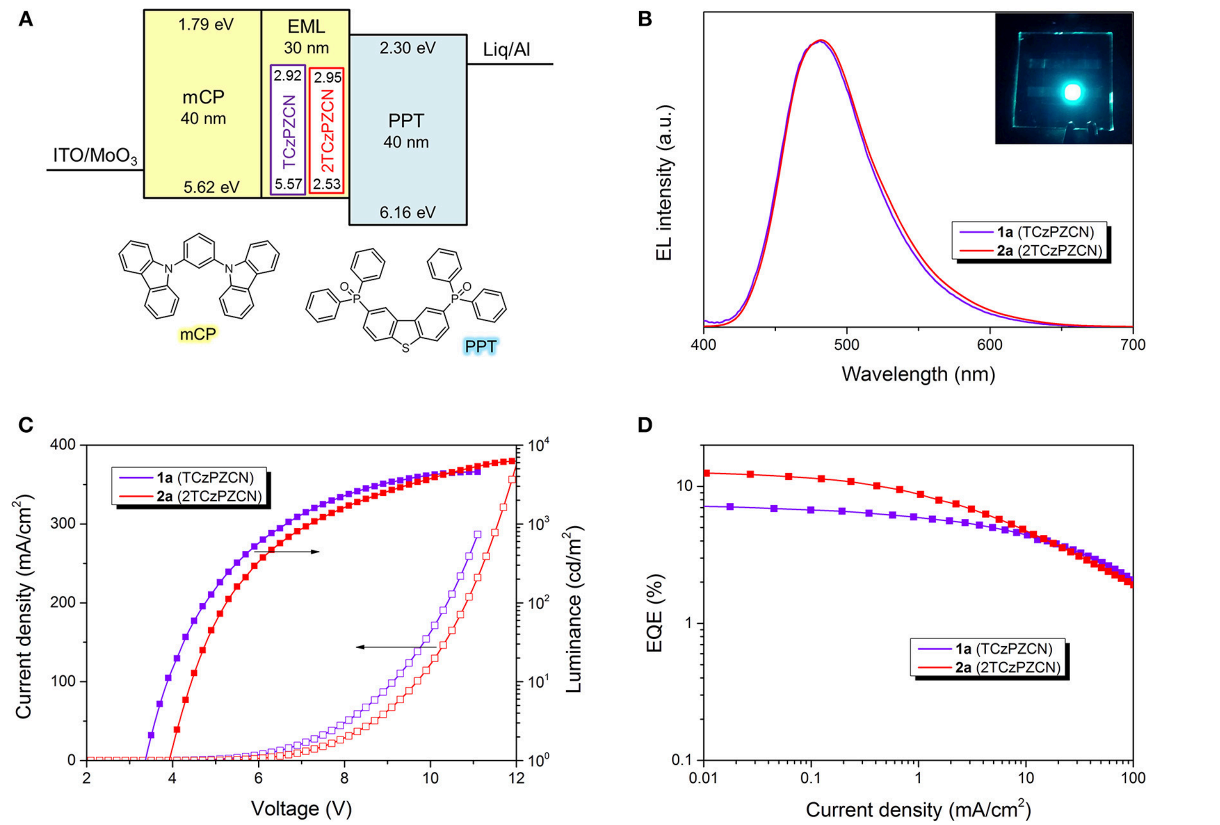

FIGURE 4 | Structures and performance of the thermally activated delayed fluorescence (TADF) organic light-emitting diodes (OLEDs). **(A)** Energy diagram of OLEDs. HOMO and LUMO levels of all compounds were measured by cyclic voltammetry. **(B)** Electroluminescence spectra at 1 mA/cm^2. Inset: The image of Device **1a**. **(C)** Luminance–current density–voltage characteristics of Devices **1a** and **2a**. **(D)** EQE–current density characteristics of Devices **1a** and **2a**.

TABLE 3 | Emissive layer (EML) component, turn-on voltage (V_{on}), maximum luminance (L_{max}), external quantum efficiency maximum (EQE_{max}), emission maximum (λ_{max}), full width at half maxima (FWHM), and CIE coordinates of the TADF OLEDs.

Device	EML	V_{on} (V)	L_{max} (cd/m^2)	EQE_{max} (%)	λ_{max} (nm)	FWHM (nm)	CIE
1a	10 wt% TCzPZCN in mCP	3.4	4,579	7.1	480	70	(0.15, 0.26)
1b	30 wt% TCzPZCN in mCP	3.2	5,339	7.6	483	73	(0.15, 0.29)
1c	neat TCzPZCN	3.3	6,053	5.4	485	80	(0.17, 0.32)
2a	10 wt% 2TCzPZCN in mCP	3.9	6,257	12.2	480	70	(0.15, 0.26)
2b	30 wt% 2TCzPZCN in mCP	3.9	7,885	10.4	489	76	(0.17, 0.35)
2c	neat 2TCzPZCN	3.7	6,375	4.9	494	80	(0.20, 0.42)

theoretical ones. In comparison to TRZ-based compounds, TCzPZCN and 2TCzPZCN have higher E_{RED} values in favor of electron injection into the emitting layers of their devices.

Six OLEDs containing TCzPZCN and 2TCzPZCN are fabricated using a very simple device structure, as shown in **Figure 4A**. The 30-nm-thick emissive layers of the six devices are TCzPZCN or 2TCzPZCN doped mCP films and their neat films (see **Table 3**). At a doping concentration of 10 wt%, both TCzPZCN- (**1a**) and 2TCzPZCN-based (**2a**) OLEDs display a sky-blue emission with a maximum at 480 nm (**Figure 4B**). Devices 1a and 2a turn-on at 3.4 and 3.9 V, respectively, and reach a maximum luminance of 4579 and 6257 cd/m2 at 11 and 12 V, respectively (**Figure 4C**). The maximum external quantum efficiencies (EQEs) of Devices **1a** and **2a** are found to be 7.1 and 12.2%, respectively (**Figure 4D**), which are both higher than the upper limit of the traditional fluorescent OLEDs (5%). Although the PLQYs of these two compounds are approximate in 10-wt%-doped mCP films, the maximum EQEs of their devices are quite different. The internal quantum efficiency (IQE) of a TADF OLED can approach the PLQY of the emitter only when the internal conversion from S_1 to S_0 is the principal deactivation pathway for the emitter (Zhang et al., 2014a). The maximum IQE for Device **1a** is lower than the PLQY of the emissive layer

(0.47) when a light out-coupling efficiency of 0.2–0.3 is assumed, indicating that the non-radiative decay at T_1 for TCzPZCN cannot be ignored in the doped films. In comparison to Device **2a**, Device **1a** shows a reduced EQE roll-off that can be attributed to the short TADF lifetime of 1.9 μs for TCzPZCN in doped film (Zhang et al., 2014a,b).

The influence of doping concentration on device performance is shown in **Figures S3**, **S4** and **Table 3**. The performance of TCzPZCN-based OLEDs is rather insensitive to the doping concentration of the emissive layer owing to the highly twisted configuration of the emitter (Zhang et al., 2015; Cha et al., 2016; Chen X.-L. et al., 2017). The electroluminescence (EL) spectra and EQE–current density curves of 10-and 30-wt%-doped devices almost coincide with each other respectively (**Figure S3**). Even the undoped device exhibits similar EQE–current density characteristics in the current density range from 1 to 100 mA/cm^2 with a slightly broader EL spectrum in comparison to the 10-wt%-doped device. In contrast, increasing the doping concentration of 2TCzPZCN-based OLEDs produces clear redshifts of the EL spectrum and decreases the EQE maximum. The lower steric hindrance surrounding the meta-linked carbazole may be responsible for the relatively strong intermolecular interaction between emitters in 2TCzPZCN doped films.

CONCLUSION

On the basis of a novel acceptor 2-cyanopyrazine, a type of blue emissive TADF molecule with small ΔE_{ST} (<0.1 eV) is successfully designed and synthesized. The fluorescence kinetics investigation indicates that the non-radiative decay rates of these molecules in toluene are far from constants. The ultrafast fluorescence decay ($1/\tau$) in the first hundred picoseconds after the excitation is related to a significant excited-state structural distortion. In doped mCP films, an *o*-phenylene-bridged 2-cyanopyrazine/3,6-di-tertbutylcarbazole compound (TCzPZCN) shows a fast TADF decay with a lifetime of 1.9 μs, as well as a high fluorescence rate of 3.7 $\times$ 10^7 s^{-1} that can be comparable to those of the TADF emitters having relatively large orbital overlap and ΔE_{ST} (>0.2 eV). Although the pyrazine-based TADF emitters in solid films exhibit only moderate quantum yields on PL and EL suffered by the structural distortion process, it is one step toward a TADF emitter with both small ΔE_{ST} and large k_F. Additionally, we have demonstrated that 2-cyanopyrazine is a promising acceptor for the construction of blue TADF emitters. By suppressing the structural distortion induced non-radiative decay, efficient pyrazine-based TADF emitters with short TADF lifetime can be expected.

DATA AVAILABILITY

The datasets generated for this study are available on request to the corresponding author.

AUTHOR CONTRIBUTIONS

All authors listed have made a substantial, direct and intellectual contribution to the work, and approved it for publication.

FUNDING

This work is supported by the National Key R&D Program of China (grant no. 2016YFB0401004) and the National Natural Science Foundation of China (grant no. 51673164, 51873183).

SUPPLEMENTARY MATERIAL

The Supplementary Material for this article can be found online at: https://www.frontiersin.org/articles/10.3389/fchem.2019.00312/full#supplementary-material

REFERENCES

Ai, X., Evans, E. W., Dong, S., Gillett, A. J., Guo, H., Chen, Y., et al. (2018). Efficient radical-based light-emitting diodes with doublet emission. *Nature* 563, 536–540. doi: 10.1038/s41586-018-0695-9

Bian, M., Zhao, Z., Li, Y., Li, Q., Chen, Z., Zhang, D., et al. (2018). Positional isomerism effect of spirobifluorene and terpyridine moieties of "$(A)_n$-D-$(A)_n$" type electron transport materials for long-lived and highly efficient TADF-PhOLEDs. *J. Mater. Chem. C* 6, 745–753. doi: 10.1039/C7TC04685E

Cai, M., Zhang, D., and Duan, L. (2018). High performance thermally activated delayed fluorescence sensitized organic light-emitting diodes. *Chem. Rec.* 18, 1–14. doi: 10.1002/tcr.201800148

Cai, X., and Su, S. J. (2018). Marching toward highly efficient, pure-blue, and stable thermally activated delayed fluorescent organic light-emitting diodes. *Adv. Funct. Mater*. 28:1802558. doi: 10.1002/adfm.201802558

Castner, E. W., Maroncelli, M., and Fleming, G. R. (1987). Subpicosecond resolution studies of solvation dynamics in polar aprotic and alcohol solvents. *J. Chem. Phys.* 86, 1090–1097. doi: 10.1063/1.452249

Cha, J.-R., Lee, C. W., Lee, J. Y., and Gong, M. S. (2016). Design of *ortho*-linkage carbazole-triazine structure for high-efficiency blue thermally activated delayed fluorescent emitters. *Dyes Pigments* 134, 562–568. doi: 10.1016/j.dyepig.2016.08.023

Chan, C.-Y., Cui, L.-S., Uk Kim, J., Nakanotani, H., and Adachi, C. (2018). Rational molecular design for deep-blue thermally activated delayed fluorescence emitters. *Adv. Funct. Mater.* 28:1706023. doi: 10.1002/adfm.201706023

Chen, D., Liu, K., Gan, L., Liu, M., Gao, K., Xie, G., et al. (2016). Modulation of exciton generation in organic active planar pn heterojunction: toward low driving voltage and high efficiency OLEDs employing conventional and thermally activated delayed fluorescent emitters. *Adv. Mater.* 28, 6758–6765. doi: 10.1002/adma.201600612

Chen, X.-K., Tsuchiya, Y., Ishikawa, Y., Zhong, C., Adachi, C., and Brédas, J. L. (2017). A new design strategy for efficient thermally activated delayed fluorescence organic emitters: from twisted to planar structures. *Adv. Mater.* 29:1702767. doi: 10.1002/adma.201702767

Chen, X.-L., Jia, J.-H., Yu, R., Liao, J.-Z., Yang, M.-X., and Lu, C. Z. (2017). Combining charge-transfer pathways to achieve unique thermally activated delayed fluorescence emitters for high-performance solution-processed, non-doped blue OLEDs. *Angew. Chem. Int. Ed.* 56, 15006–15009. doi: 10.1002/anie.201709125

Chen, Z., Wu, Z., Ni, F., Zhong, C., Zeng, W., Wei, D., et al. (2018). Emitters with a pyridine-3,5-dicarbonitrile core and short delayed fluorescence lifetimes of about 1.5 μs: orange-red TADF-based OLEDs with very slow efficiency roll-offs at high luminance. *J. Mater. Chem. C* 6, 6543–6548. doi: 10.1039/C8TC01698D

Cui, L.-S., Nomura, H., Geng, Y., Kim, J. U., Nakanotani, H., and Adachi, C. (2017). Controlling singlet–triplet energy splitting for deep-blue thermally activated delayed fluorescence emitters. *Angew. Chem. Inter. Ed.* 56, 1571–1575. doi: 10.1002/anie.201609459

Deng, C., Zhang, L., Wang, D., Tsuboi, T., and Zhang, Q. (2019). Exciton- and polaron-induced reversible dipole reorientation in amorphous organic semiconductor films. *Adv. Opt. Mater.* 7:1801644. doi: 10.1002/adom.201801644

Endo, A., Sato, K., Yoshimura, K., Kai, T., Kawada, A., Miyazaki, H., et al. (2011). Efficient up-conversion of triplet excitons into a singlet state and its application for organic light emitting diodes. *Appl. Phys. Lett.* 98:083302. doi: 10.1063/1.3558906

Ganesan, P., Ranganathan, R., Chi, Y., Liu, X.-K., Lee, C.-S., Liu, S.-H., et al. (2017). Functional pyrimidine-based thermally activated delay fluorescence emitters: photophysics, mechanochromism, and fabrication of organic light-emitting diodes. *Chem. Eur. J.* 23, 2858–2866. doi: 10.1002/chem.201604883

Gao, B., Zhou, Q., Geng, Y., Cheng, Y., Ma, D., Xie, Z., et al. (2006). New fluorescent dipolar pyrazine derivatives for non-doped red organic light-emitting diodes. *Mater. Chem. Phys.* 99, 247–252. doi: 10.1016/j.matchemphys.2005.10.020

Gómez-Bombarelli, R., Aguilera-Iparraguirre, J., Hirzel, T. D., Duvenaud, D., Maclaurin, D., Blood-Forsythe, M. A., et al. (2016). Design of efficient molecular organic light-emitting diodes by a high-throughput virtual screening and experimental approach. *Nat. Mater.* 15, 1120–1127. doi: 10.1038/nmat4717

Hirata, S., Sakai, Y., Masui, K., Tanaka, H., Lee, S. Y., Nomura, H., et al. (2015). Highly efficient blue electroluminescence based on thermally activated delayed fluorescence. *Nat. Mater.* 14, 330–336. doi: 10.1038/nmat4154

Huang, S., Zhang, Q., Shiota, Y., Nakagawa, T., Kuwabara, K., Yoshizawa, K., et al. (2013). Computational prediction for singlet- and triplet-transitionEnergies of charge-transfer compounds. *J. Chem. Theory Comput.* 9, 3872–3877. doi: 10.1021/ct400415r

Kaji, H., Suzuki, H., Fukushima, T., Shizu, K., Suzuki, K., Kubo, S., et al. (2015). Purely organic electroluminescent material realizing 100% conversion from electricity to light. *Nat. Comm.* 6:8476. doi: 10.1038/ncomms9476

Kinoshita, S., and Nishi, N. (1988). Dynamics of fluorescence of a dye molecule in solution. *J. Chem. Phys.* 89, 6612–6622. doi: 10.1063/1.455383

Komatsu, R., Sasabe, H., Seino, Y., Nakao, K., and Kido, J. (2016). Light-blue thermally activated delayed fluorescent emitters realizing a high external quantum efficiency of 25% and unprecedented low drive voltages in OLEDs. *J. Mater. Chem. C* 4, 2274–2278. doi: 10.1039/C5TC04057D

Lee, C. W., and Lee, J. Y. (2015). Systematic control of photophysical properties of host materials for high quantum efficiency above 25% in green thermally activated delayed fluorescent devices. *ACS Appl. Mater. Interfaces* 7, 2899–2904. doi: 10.1021/am508259u

Lee, S. Y., Yasuda, T., Nomura, H., and Adachi, C. (2012). High-efficiency organic light-emitting diodes utilizing thermally activated delayed fluorescence from triazine-based donor-acceptor hybrid molecules. *Appl. Phys. Lett.* 101:093306. doi: 10.1063/1.4749285

Li, B., Nomura, H., Miyazaki, H., Zhang, Q., Yoshida, K., Suzuma, Y., et al. (2014). Dicarbazolyldicyanobenzenes as thermally activated delayed fluorescence emitters: effect of substitution position on photoluminescent and electroluminescent Properties. *Chem. Lett.* 43, 319–321. doi: 10.1246/cl.130907

Li, C., Duan, R., Liang, B., Han, G., Wang, S., Ye, K., et al. (2017). Deep-red to near-infrared thermally activated delayed fluorescence in organic solid films and electroluminescent devices. *Angew. Chem. Int. Ed.* 56, 11525–11529. doi: 10.1002/anie.201706464

Li, J., Nakagawa, T., MacDonald, J., Zhang, Q., Nomura, H., Miyazaki, H., et al. (2013). Highly efficient organic light-emitting diode based on a hidden thermally activated delayed fluorescence channel in a heptazine derivative. *Adv. Mater.* 25, 3319–3323. doi: 10.1002/adma.201300575

Li, W., Pan, Y., Yao, L., Liu, H., Zhang, S., Wang, C., et al. (2014). A hybridized local and charge-transfer excited state for highly efficient fluorescent OLEDs: molecular design, spectral character, and full exciton utilization. *Adv. Opt. Mater.* 2, 892–901. doi: 10.1002/adom.201400154

Lin, T.-A., Chatterjee, T., Tsai, W.-L., Lee, W.-K., Wu, M.-J., Jiao, M., et al. (2016). Sky-blue organic light emitting diode with 37% external quantum efficiency using thermally activated delayed fluorescence from spiroacridine-triazine hybrid. *Adv. Mater.* 28, 6976–6983. doi: 10.1002/adma.201601675

Liu, Y., Li, C., Ren, Z., Yan, S., and Bryce, M. R. (2018). All-organic thermally activated delayed fluorescence materials for organic light-emitting diodes. *Nat. Rev. Mater.* 3, 1–20. doi: 10.1038/natrevmats.2018.20

Liu, Z., Cao, F., Tsuboi, T., Yue, Y., Deng, C., Ni, X., et al. (2018). A high fluorescence rate is key for stable blue organic light-emitting diodes, *J. Mater. Chem. C* 6, 7728–7733. doi: 10.1039/C8TC01471J

Liu, Z., Qiu, J., Wei, F., Wang, J., Liu, X., Helander, M., et al. (2014). Simple and high efficiency phosphorescence organic light-emitting diodes with codeposited copper(I) emitter. *Chem. Mater.* 26, 2368–2373. doi: 10.1021/cm5006086

Mazur, U., and Hipps, K. W. (1995). Resonant tunneling bands and electrochemical reduction potentials. *J. Phys. Chem.* 99, 6684–6688. doi: 10.1021/j100017a060

Nakao, K., Sasabe, H., Komatsu, R., Hayasaka, Y., Ohsawa, T., and Kido, J. (2017). Significant enhancement of blue OLED performances through molecular engineering of pyrimidine-based emitter. *Adv. Opt. Mater.* 5:1600843. doi: 10.1002/adom.201600843

Oh, C. S., de Sa Pereira, D., Han, H., Park, H. J., Higginbotham, H. F., Monkman, A. P., et al. (2018). Dihedral angle control of blue thermally activated delayed fluorescent emitters through donor substitution position for efficient reverse intersystem crossing. *ACS Appl. Mater. Interfaces* 10, 35420–35429. doi: 10.1021/acsami.8b10595

Pan, K.-C., Li, S.-W., Ho, Y.-Y., Shiu, Y.-J., Tsai, W.-L., Jiao, M., et al. (2016). Efficient and tunable thermally activated delayed fluorescence emitters having orientation-adjustable CN-substituted pyridine and pyrimidine acceptor units. *Adv. Funct. Mater.* 26, 7560–7571. doi: 10.1002/adfm.201602501

Park, S., Komiyama, H., and Yasuda, T. (2017). Pyrimidine-based twisted donor–acceptor delayed fluorescence molecules: a new universal platform for highly efficient blue electroluminescence. *Chem. Sci.* 8, 953–960. doi: 10.1039/C6SC03793C

Phifer, C. C., and McMillin, D. R. (1986). The basis of aryl substituent effects on charge-transfer absorption intensities. *Inorg. Chem.* 25, 132–1333. doi: 10.1021/ic00229a008

Rajamalli, P., Senthilkumar, N., Huang, P.-Y., Ren-Wu, C.-C., Lin, H.-W., and Cheng, C.- H. (2017). New molecular design concurrently providing superior pure blue, thermally activated delayed fluorescence and optical out-coupling efficiencies. *J. Am. Chem. Soc.* 139, 10948–10951. doi: 10.1021/jacs.7b03848

Sasabe, H., Onuma, N., Nagai, Y., Ito, T., and Kido, J. (2017). High power efficiency blue-to-green organic light-emitting diodes using isonicotinonitrile-based fluorescent emitters. *Chem. Asian J.* 12, 648–654. doi: 10.1002/asia.201601641

Shao, S., Hu, J., Wang, X., Wang, L., Jing, X., and Wang, F. (2017). Blue thermally activated delayed fluorescence polymers with nonconjugated backbone and through-space charge transfer effect. *J. Am. Chem. Soc.* 139, 17739–17742. doi: 10.1021/jacs.7b10257

Sommer, G. A., Mataranga-Popa, L. N., Czerwieniec, R., Hofbeck, T., Homeier, H. H. H., Muller, T. J., et al. (2018). Design of conformationally distorted donor-acceptor dyads showing efficient thermally activated delayed fluorescence. *J. Phys. Chem. Lett.* 9, 3692–3697. doi: 10.1021/acs.jpclett.8b01511

Sun, H., Hu, Z., Zhong, C., Chen, X., Sun, Z., and Bredas, J.- L. (2017). Impact of dielectric constant on the singlet-triplet gap in thermally activated delayed fluorescence materials. *J. Phys. Chem. Lett.* 8, 2393–2398. doi: 10.1021/acs.jpclett.7b00688

Tanaka, H., Shizu, K., Miyazaki, H., and Adachi, C. (2012). Efficient green thermally activated delayed fluorescence (TADF) from a phenoxazine-triphenyltriazine (PXZ-TRZ) derivative. *Chem. Comm.* 48, 11392–11394. doi: 10.1039/c2cc36237f

Taneda, M., Shizu, K., Tanaka, H., and Adachi, C. (2015). High efficiency thermally activated delayed fluorescence based on 1,3,5-tris(4-(diphenylamino)phenyl)-2,4,6-tricyanobenzene. *Chem. Comm.* 51, 5028–5031. doi: 10.1039/C5CC00511F

Tang, C., Yang, T., Cao, X., Tao, Y., Wang, F., Zhong, C., et al. (2015). Tuning a weak emissive blue host to highly efficient green dopant by a CN in tetracarbazolepyridines for solution-processed thermally activated delayed fluorescence devices. *Adv. Opt. Mater.* 3, 786–790. doi: 10.1002/adom.201500016

Turro, N. J., Ramamurthy, V., and Scaiano, J. C. (2010). *Modern Molecular Photochemistry of Organic Molecules.* Sausalito, CA: University Science Books.

Uoyama, H., Goushi, K., Shizu, K., Nomura, H., and Adachi, C. (2012). Highly efficient organic light-emitting diodes from delayed fluorescence. *Nature* 492, 234–238. doi: 10.1038/nature11687

Wang, C., Deng, C., Wang, D., and Zhang, Q. (2018). Prediction of Intramolecular charge-transfer excitation for thermally activated delayed fluorescence molecules from a descriptor-tuned density functional. *J. Phys. Chem. C* 122, 7816–7823. doi: 10.1021/acs.jpcc.7b10560

Wang, C., and Zhang, Q. (2019). Understanding solid-state solvation-enhanced thermally activated delayed fluorescence using a descriptor-tuned screened range-separated functional. *J. Phys. Chem. C* 123, 4407–4416. doi: 10.1021/acs.jpcc.8b08228

Wang, D., Huang, S., Wang, C., Yue, Y., and Zhang, Q. (2019). Computational prediction for oxidation and reduction potentials of organic molecules used in organic light-emitting diodes. *Org. Electron.* 64, 216–222. doi: 10.1016/j.orgel.2018.10.038

Wang, H., Xie, L., Peng, Q., Meng, L., Wang, Y., Yi, Y., et al. (2014). Novel thermally activated delayed fluorescence materials–thioxanthone derivatives and their applications for highly efficient OLEDs. *Adv. Mater.* 26, 5198–5204. doi: 10.1002/adma.201401393

Wang, K., Zheng, C.-J., Liu, W., Liang, K., Shi, Y.-Z., Tao, S.-L., et al. (2017). Avoiding energy loss on TADF emitters: controlling the dual conformations of D–A structure molecules based on the pseudoplanar segments. *Adv. Mater.* 29:1701476. doi: 10.1002/adma.201701476

Wang, Q., Zhang, Y.-X., Yuan, Y., Hu, Y., Tian, Q.-S., Jiang, Z.-Q., et al. (2019). Alleviating efficiency roll-off of hybrid single-emitting layer WOLED utilizing bipolar TADF material as host and emitter. *ACS Appl. Mater. Interfaces* 11, 2197–2204. doi: 10.1021/acsami.8b18665

Wang, R., Wang, Y.-L., Lin, N., Zhang, R., Duan, L., and Qiao, J. (2018). Effects of ortho-linkages on the molecular stability of organic light-emitting diode materials. *Chem. Mater.* 30, 8771–8781. doi: 10.1021/acs.chemmater.8b03142

Wex, B., and Kaafarani, B. R. (2017). Perspective on carbazole-based organic compounds as emitters and hosts in TADF applications. *J. Mater. Chem. C* 5, 8622–8653. doi: 10.1039/C7TC02156A

Wu, K., Zhang, T., Zhan, L., Zhong, C., Gong, S., Jiang, N., et al. (2016). Optimizing optoelectronic properties of pyrimidine-based TADF emitters by changing the substituent for organic light-emitting diodes with external quantum efficiency close to 25% and slow efficiency Roll-Off. *Chem. Eur. J.* 22, 10860–10866. doi: 10.1002/chem.201601686

Wu, T.-L., Huang, M.-J., Lin, C.-C., Huang, P.-Y., Chou, T.-Y., Chen-Cheng, R.-W., et al. (2018). Diboron compound-based organic light-emitting diodes with high efficiency and reduced efficiency roll-off. *Nat. Photonics* 12, 235–240. doi: 10.1038/s41566-018-0112-9

Xiang, Y., Zhao, Y., Xu, N., Gong, S., Ni, F., Wu, K., et al. (2017). Halogen-induced internal heavy-atom effect shortening the emissive lifetime and improving the fluorescence efficiency of thermally activated delayed fluorescence emitters. *J. Mater. Chem. C* 5, 12204–12210. doi: 10.1039/C7TC04181K

Yang, Z., Mao, Z., Xie, Z., Zhang, Y., Liu, S., Zhao, J., et al. (2017). Recent advances in organic thermally activated delayed fluorescence materials. *Chem. Soc. Rev.* 46, 915–1016. doi: 10.1039/C6CS00368K

Yuan, Y., Hu, Y., Zhang, Y.-X., Lin, J.-D., Wang, Y.-K., Jiang, Z.-Q., et al. (2017). Light-emitting diodes: Over 10% EQE near-infrared electroluminescence based on a thermally activated delayed fluorescence emitter. *Adv. Funct. Mater.* 27:1700986. doi: 10.1002/adfm.201700986

Zhang, D., Cai, M., Zhang, Y., Zhang, D., and Duan, L. (2016). Sterically shielded blue thermally activated delayed fluorescence emitters with improved efficiency and stability. *Mater. Horiz.* 3, 145–151. doi: 10.1039/C5MH00258C

Zhang, D., Song, X., Cai, M., Kaji, H., and Duan, L. (2018). Versatile indolocarbazole-isomer derivatives as highly emissive emitters and ideal hosts for thermally activated delayed fluorescent OLEDs with alleviated efficiency roll-off. *Adv. Mater.* 30:1705406. doi: 10.1002/adma.201705406

Zhang, D.-D., Suzuki, K., Song, X.-Z., Wada, Y., Kubo, S., Duan, L., et al. (2019). Thermally activated delayed fluorescent materials combining intra- and intermolecular charge transfers. *ACS Appl. Mater. Interfaces* 11, 7192–7198. doi: 10.1021/acsami.8b19428

Zhang, Q., Kuwabara, H., Potscavage, W. J., Huang, S., Hatae, Y., Shibata, T., et al. (2014a). Anthraquinone-based intramolecular charge-transfer compounds: computational molecular design, thermally activated delayed fluorescence, and highly efficient red electroluminescence. *J. Am. Chem. Soc.* 136, 18070–18081. doi: 10.1021/ja510144h

Zhang, Q., Li, B., Huang, S., Nomura, H., Tanaka, H., and Adachi, C. (2014b). Efficient blue organic light-emitting diodes employing thermally activated delayed fluorescence. *Nat. Photonics* 8, 326–332. doi: 10.1038/nphoton.2014.12

Zhang, Q., Li, J., Shizu, K., Huang, S., Hirata, S., Miyazaki, H., et al. (2012). Design of efficient thermally activated delayed fluorescence materials for pure blue organic light emitting diodes. *J. Am. Chem. Soc.* 134, 14706–14709. doi: 10.1021/ja306538w

Zhang, Q., Tsang, D., Kuwabara, H., Hatae, Y., Li, B., Takahashi, T., et al. (2015). Nearly 100% internal quantum efficiency in undoped electroluminescent devices employing pure organic emitters. *Adv. Mater.* 27, 2096–2100. doi: 10.1002/adma.201405474

Zhang, Q., Xiang, S., Huang, Z., Sun, S., Ye, S., Lv, X., et al. (2018). Molecular engineering of pyrimidine-containing thermally activated delayed fluorescence emitters for highly efficient deep-blue (CIEy $<$ 0.06) organic light-emitting diodes. *Dyes Pigments* 155, 51–58. doi: 10.1016/j.dyepig.2018.03.004

Zhu, Y., Zhang, Y., Yao, B., Wang, Y., Zhang, Z., Zhan, H., et al. (2016). Synthesis and electroluminescence of a conjugated polymer with thermally activated delayed fluorescence. *Macromolecules* 49, 4373–4377. doi: 10.1021/acs.macromol.6b00430

Conflict of Interest Statement: The authors declare that the research was conducted in the absence of any commercial or financial relationships that could be construed as a potential conflict of interest.